Immunolocalization of Basic Fibroblast Growth Factor and Platelet-Derived Growth Factor-A During Adjuvant Arthritis in the Lewis Rat

Zhenhong Qu,* Marcia Picou,†
Thao Tran Dang,†Ethen Angell,†
Stephen R. Planck,†‡ Charles E. Hart,§ and
James T. Rosenbaum*†‡

From the Departments of Cell Biology and Anatomy,
Medicine,† and Ophthalmology,‡ The Oregon Health
Sciences University, Casey Eye Institute, Portland, Oregon;
and ZymoGenetics, Inc.,§ Seattle, Washington*

A prerequisite in defining the role of a growth factor in a disease is knowledge of its expression kinetics during the natural course of the disease. We, therefore, used immunohistochemical and immunoblot analyses to examine tissue distribution of basic fibroblast growth factor (bFGF) and platelet-derived growth factor (PDGF-A) during the development of destructive arthropathy in the rat adjuvant arthritis model. In normal joints, bFGF was primarily localized in endothelial cells. In inflamed joints, increased staining for bFGF was found in the invading panni, hyperplastic synovium, and thickened periosteum where bFGF was also co-localized with two cell proliferation markers. Staining for bFGF began to increase at the onset of arthritis (days 11 to 13), reached peak level on days 17 to 24, and gradually declined afterward. In contrast, PDGF-A staining did not change until day 17 and the increased staining was restricted to areas of newly formed bone. The distinct temporal and spatial distribution pattern of these two growth factors during the destructive arthropathy strongly suggests that they play different roles during arthritis. Although PDGF-A seems to be exclusively related to osteogenesis, bFGF may have a more extensive impact on synovial proliferation and bone destruction as well as bone formation. (Am J Pathol 1994, 145:1127–1139)

Rheumatoid arthritis (RA) is an immunologically mediated chronic disorder characterized by invasive growth of inflamed synovial tissue that leads to joint destruction. The mechanism underlying this disease is largely unknown. Increasing evidence indicates that growth factors (GFs) and cytokines are involved in RA.[1,2] Of these GFs, basic fibroblast growth factor (bFGF) is of particular interest. It is a potent mitogenic, angiogenic, and chemotactic factor and has been implicated in the wound-healing processes,[3–7] which exhibit resemblance to aspects of RA. Recent studies seem to support the hypothesis that bFGF is involved in RA. bFGF is a potent inducer of a variety of metalloproteinases[8,9] and plasminogen activator.[10] It up-regulates interleukin-1 (IL-1) receptor expression in chondrocytes[11] and thereby potentiates IL-1-induced metalloproteinase production.[8] It also synergizes with tumor necrosis factor (TNF)-α in inducing the synthesis of matrix proteinases and the release of proteinases from synovial fibroblasts.[12] bFGF alone or synergizing with IL-1 induces synthesis and release of prostaglandin E by articular chondrocytes and rheumatoid synovial cells.[8,13–15] The findings that repeated intraarticular injection of IL-1 results in a chronic synovitis without cartilage and bone destruction,[16] whereas co-injection of IL-1 and bFGF induces degradation of articular cartilage,[17] suggest an important role of bFGF in cartilage and bone destruction. Unlike other GFs or cytokines detected in arthritic joint tissue such as IL-1 or TNF-α, bFGF seems to be involved not only in the destructive process but also in wound repair. It also has been implicated in bone formation *in vitro* and *in vivo*.[18–21] We and others reported that cultured synoviocytes also synthesize, bind, and proliferate in response to bFGF.[22,23] Two recent studies show that inhibition of nitric oxide synthesis results in suppression of arthritis

in Lewis rats and that bFGF markedly inhibits interferon-γ/endotoxin-induced nitric oxide synthase.[24,25] Thus, bFGF may have dual effects on articular inflammation. It may play a role in destructive changes; it may also be involved in the wound repair process and have beneficial effects in protecting joint tissue from inflammatory attack. In view of the simultaneous presence of both tissue destruction and repair in RA, we were intrigued to examine bFGF expression in relation to disease processes and pathological changes.

To better define the role of a GF in a disease process, it is very important to examine the temporal expression and localization of the growth factor during the initiation and development of the disease. However, efforts made to characterize the pathophysiological roles of GFs during rheumatoid changes *in vivo* are often hampered by three major obstacles. First, the detection of a GF cannot be equated with proof that it plays a causal role. Second, synovial samples used for immunolocalization of growth factors are largely obtained from patients with long-established disease. It is, therefore, unclear whether the expression of a GF in the tissue samples is a primary (ie, causal) or secondary (ie, resultant) event. Third, medication has the potential to modulate expression of GFs. We therefore used a well-characterized arthritis animal model[26,27] to investigate the expression kinetics of bFGF in joint tissues in relation to pathological changes during the development of adjuvant arthritis. We focused on bone destruction in synovium-cartilage junction (SCJ) and osteogenesis. Because up-regulated expression of multiple GFs appears to be a common occurrence during articular inflammation, we used platelet-derived growth factor (PDGF-A), a GF with considerable functional overlap with bFGF for comparison. Our results show that in contrast to immunostaining for PDGF-A, increased bFGF staining coincides with active cell proliferation, invasive growth of panni, and bone formation, suggesting that bFGF may play an important role during articular inflammation.

Materials and Method

Induction of Adjuvant Polyarthritis

Pathogen-free female Lewis rats (Harlan Sprague-Dawley, Indianapolis, IN) at 170 to 200 were used for this study. The animals were kept for at least 2 days under constant environmental conditions with food and water ad libitum before experimentation. All the experiments were performed in accordance with the guidelines approved by the Committee for Care and Use of Laboratory Animals at the Oregon Health Sciences University.

Adjuvant arthritis was induced by intradermal injection of 1 to 1.5 mg of mycobacterium butyricum (Difco, Detroit, MI) suspended in mineral oil (10 mg/ml) (Sigma, St. Louis, MO) into the tail base. The extent of arthritis was quantitated by volumetric measurement of each of the two hind feet, as determined by immersion of each in fluid up to a tattoo mark 5 mm above each ankle. The amount of water displaced served as a quantitation of limb swelling. The severity of arthritis in each hind limb was scored as the percentage increase in volume:

$$\text{Arthritic Score} = \left(\frac{V_2}{V_1} - 1 \right) \times 100$$

where V1 represents the volume of the limb on the initial measurement on day 0, whereas V2 represents the measurement on sacrifice. Results from repeated measurements over 84 ankle joints in our pilot study showed that the error of measurement was 4.5 ± 2.4%. The maximal increase of the score in normal rat as a result of natural growth in a 40-day period was less than 15%.

Rats were sacrificed by CO_2 inhalation on day 9 and at 5- to 7-day intervals starting at days 11 to 13 (onset) after tail injection (Table 1). Untreated rats (n = 4) were used as control. Intraperitoneal injection of bromodeoxyuridine (BrdU) at 50 mg/kg and fluorodeoxyuridine (FldU) at 5 mg/ml was given 2 to 3 hours before sacrifice for pulse labeling of proliferating cells. Afflicted hind limbs with typical arthritic scores were selected at each time point and used for this study. Hind limbs with arthritic scores ≤15% (n = 7) from five adjuvant-treated rats were considered as arthritis free and were also examined.

Processing of the Tissues

For immunohistochemical study, afflicted hind limbs were amputated above the malleolus and the middle of the metatarsals after the skin was peeled off. The samples were fixed in Bouin's solution for 1 to 2 days at 4 C and then decalcified in 0.1 M Tris buffer (pH 7.2) containing 10% EDTA with daily changes for 20 to 25 days. After extensive washing in Tris buffer, the tissues underwent routine processing until embedded in paraffin. Immunohistochemical localization of bFGF and PDGF-A was conducted using the paraffin sections. To identify the actively proliferating cells, the tissue sections were also stained for proliferating cell nuclear antigen (PCNA) and BrdU.

Table 1. *Summary of Pathological Changes During Arthritic Inflammation*

Day	Control	9	11–13	17–20	22–27	33–40
n	4	5	6	24	11	5
Score range	0	0–10	30–60	60–80	60–80	50–80
Major pathological changes						
Periosteum (cell layer)	1–2	1–21	Hypertrophy	Hyperplasia	Hyperplasia	2–4
Infiltration	–	–	+	++	+++	++
Neovascularization	–	–	++	+++	+++	+
Pannus formation	–	–	–	+	+++	NA
Bone destruction	–	–	+	++	+++	NA
Osteogenesis	–	–	–	+	++	+++
bFGF/PDGF-A immunostaining						
Synovium	–/–	–/–	+/–	++/–	++/–	+/–
Periosteum	–/–	–/–	++/–	+++/–	+++/–	+/–
Pannus	NA	NA	NA	+++/–	+++/–	+/–
Osteogenic tissue	NA	NA	NA	++/+	++/++	+/+++
bFGF staining at SCJs (Mean + SD%)						
Intact SCJs	13.2 ± 6.3	17.1 ± 10.3	56.1 ± 14.9	78.1 ± 18.4	80.6 ± 10.1	NA
Eroded SCJs	NA	NA	87.5 ± 9.8	87.2 ± 11.3	88.1 ± 9.2	NA
Total SCJs	13.2 ± 6.3	17.1 ± 10.3	63.7 ± 9.1	81.8 ± 9.2	86.5 ± 10.5	NA

Infiltration: infiltrated cells per field at 400X 20 to 50 = +, 50 to 200 = ++, >200 = +++.
Neovascularization: small vessels per field at 400X 3 to 5 = +, 5 to 8 = ++, >8 = +++.
Bone destruction: ratio of thickness of replaced and original cortex <1/2 = +, 1 = ++, >1 = +++.
Osteogenesis: ratio of thickness of newly formed bone/original cortex ≤1/2 = +, 1 = ++, >1 = +++.
Immunostaining: weak +, moderate ++, strong +++.
NA, not applicable.

For Western blot analysis of bFGF-like molecules, the hind limbs were dissected skin-free and immediately snap-frozen and stored in liquid nitrogen. To extract total protein from the joint tissues, the samples were ground into powder in liquid nitrogen and dissolved in a lysis buffer (pH 7.3) containing 25 mmol/L HEPES, 0.4 M NaCl, 2 mmol/L MgCl, 1% NP-40, 2 mmol/L phenylmethylsulfonylfluoride (PMSF), 1 mmol/L leupeptin, and 1 mmol/L aprotinin. The samples were homogenized with a Brinkmann PT3000 Polytron (Dispergir-und Mischtechnik, Luzern, Switzerland) at maximal speed for four 30-second pulses. After centrifugation at 1000 × *g* for 5 minutes, the supernatant was collected. To ensure maximal yield of soluble proteins, the pellets were dissolved in fresh lysis buffer and the extraction was repeated twice. The supernatants from repeated extractions were collected, mixed well, and the total protein was measured by Pierce BCA Protein Assay following the vendor's instruction (no. 23209; Pierce, Rockford, IL). The samples were then stored at –70 C until use.

Immunohistochemical Staining for bFGF, PDGF, and PCNA

Immunohistochemical staining used for this study was as previously described.[28] Briefly, paraffin-embedded tissues were cut into 4 to 6 μ sections and laid on poly-L-lysine-coated slides. To improve adherence, the slides were heated at 60 C for 30 minutes in a humid chamber. The sections were deparaf-finized in xylene and rehydrated through graded series of alcohol and distilled water. A brief enzymatic treatment was conducted when necessary to retrieve the antigenicity (Table 2). To block nonspecific antibody binding, the sections were incubated in phosphate-buffered saline (PBS) containing 0.3% bovine serum albumin (BSA) and 1% normal goat and horse sera for 20 minutes. A three-step avidin-biotin complex (ABC) protocol was used for staining unless otherwise specified. After washing and blocking steps, the slides were incubated with a primary antibody at an appropriate dilution (Table 2) overnight at 4 C. Then, a biotinylated goat anti-rabbit or horse anti-mouse secondary antibody (adsorbed with rat serum) was applied at 1:200 for 40 minutes followed by incubation with alkaline phosphatase (AP)-or horseradish peroxidase (HRP)-conjugated ABC for 30 minutes, according to the vendor's instructions (Vector Laboratories, Burlingame, CA). The antibody-antigen complexes were visualized by incubation for 30 minutes in Fast Red substrate containing 2 mmol/L levamisole (BioGenex Laboratories, San Ramon, CA), according to the supplier's instructions or by incubation for 10 minutes with a HRP substrate solution containing 0.5 mg/ml 3,3'-diaminobenzidine (DAB), 0.1 M imdazole, and 0.03% H_2O_2 in PBS. The sections were counterstained with Gill III hematoxylin and mounted in Crystal Mount (Biømeda Corp., Foster City, CA).

For bFGF staining with the mouse monoclonal antibody, a two-step indirect staining method was also used. After incubation with the monoclonal antibody

Table 2.   *List of Primary Antibodies Used in this Study*

Antibody	Species	Dilution Concentration	Treatment	Source
Anti-bFGF	Mouse*	1:20,000 (<3 µg/ml)	Hyaluronidase	ZymoGenetics Inc., Seattle WA
Anti-bFGF	Rabbit IgG	1:500 (2 µg/ml)	Hyaluronidase	Biomedical Technologies Inc., Stoughton, MA
Anti-BrdU	Mouse IgG	1:100 (0.5 µg/ml)	Pepsin/HCl	Becton Dickenson, San Jose, CA
Anti-PCNA	Mouse IgG	1:100 (3.7 µg/ml)	None	Dako Corp., Carpinteria, CA
Anti-PDGF-A[†]	Rabbit IgG	1:500 (1.4 µg/ml)	Pepsin	ZymoGenetics

*This antibody is raised against full molecules of human recombinant bFGF and does not cross-react with acidic FGF on immunoblot analysis.[46] Clone number of this antibody is 148.6.1.1.1. The listed dilution is for two-step indirect method. For ABC method, the dilution is 1:10[6] (<0.1 µg/ml).

[†]The antibody is rased against human recombinant PDGF-A and is cross-adsorbed with PDGF-B. No cross-rection with PDGF-B is observed.[47]

to bFGF at 1:20,000 for 1 hour and then two brief washes in PBS, the sections were incubated with an AP-conjugated goat anti-mouse IgG (GIBCO BRL, Grand Island, NY) at 1:100 in the diluting buffer containing 5% normal rat serum for 30 minutes. The antigen-antibody complexes were visualized by Fast Red as described above.

The control groups included: 1) replacing the specific primary antibodies with nonimmune IgG at the same concentration from the same species; 2) preincubation of a primary antibody with the specific antigen before staining for bFGF and PDGF-A; 3) for bFGF staining, washing the sections with PBS containing 2 M NaCl after enzymatic treatment; and 4) for BrdU staining, tissue samples from rat not injected with BrdU.

Double or Triple Labeling of bFGF, PDGF, and PCNA/BrdU

For double labeling of PCNA and bFGF, tissue sections were stained first for PCNA using the ABC-HRP method with DAB as substrate. A two-step indirect method was used for bFGF staining, as described above with Fast Red as substrate.

To determine the spatial correlation of bFGF and PDGF-A, double immunolabeling was performed in which the sections were stained first for bFGF using the ABC-AP method and Fast Red as substrate. Staining of PDGF-A was then conducted using the ABC-HRP method with DAB as substrate as described above.

For triple labeling, the sections after bFGF/PDGF-A double staining were treated with 2 N HCl for 15 minutes at room temperature and incubated with PBS containing 0.3% BSA and 1% normal goat and horse serum for 20 minutes. The samples were then incubated with anti-BrdU at 1:20 for 1 hour followed by incubation with FITC-conjugated goat anti-mouse IgG at 1:50 containing 5% of normal rat serum for 40 minutes.

Assessment of bFGF Staining in Relation to Joint Destruction and Cell Proliferation

To determine a correlation between GF staining and joint destruction, the number of SCJs with bFGF staining was counted by two investigators independently (one was blinded to the tissue samples). The frequencies of bFGF and PDGF-A staining at both intact and damaged SCJs of all joints in a limb were then compared with control. The number of periosteal cells stained positive for PCNA/BrdU was also counted and expressed as a percentage. The data were analyzed with Students' *t*-test and the frequency was expressed as mean ± standard SD.

Western Blot Analysis of bFGF-Like Molecules

The joint tissue lysates were analyzed for bFGF-like proteins by Western blot analysis using the mouse monoclonal antibody (148.6.1.1.1) (Table 2). Briefly, 1 mg of total protein from each sample was precleaned by incubation with 20 µl of protein G/protein A agarose (IP05, Oncogene Science, Uniondale, NY) for 3 hours with agitation at room temperature. After brief centrifugation, the sample supernatant was transferred into new 1.75-ml tubes containing 15 µl of heparin acrylic beads (H-5263 Sigma) that had been washed with the lysis buffer containing 3 M NaCl at pH 7.4 and equilibrated with lysis buffer. The sample was incubated with the beads overnight at 4 C. The heparin beads were washed twice with the lysis buffer containing 0.6 M NaCl and equilibrated with 10 mmol/L HEPES at pH 7.4. The beads were collected by brief centrifugation, resuspended in 30 µl of sodium dodecyl sulfate (SDS) electrophoresis sample buffer (0.125 M Tris, 4% SDS, 30% glycerol, and 2% 2-mercaptoethanol), and subjected to electrophoresis in 15% polyacrylamide gels. The separated proteins were transferred onto PVDF membranes at 95 V for 60

minutes at 10 to 12 C in a Hoefer electroblotting tank (Hoefer Scientific Instruments, San Francisco, CA). A modified buffer containing 50 mmol/L Tris base, 48 mmol/L glycine, 10% methanol, and 0.02% SDS, pH 9.3, at 10 C was used to optimize the transfer and binding efficiency of bFGF. The transferring efficiency of bFGF to the membrane was monitored by silver staining of the polyacrylamide gel after blotting, according to the method of Wray et al[29] and by immunostaining a second layer of PVDF membrane. For a negative control, beads incubated with samples were washed with a 2 M NaCl buffer to remove the bound bFGF before adding electrophoresis sample buffer-.Human recombinant bFGF was used as a positive control with or without incubation with heparin beads.

Nonspecific binding to blot was blocked with PBS containing 5% normal horse serum, 2% nonfat milk, and 2% BSA for 1 hour at room temperature. The blot was incubated with the monoclonal anti-bFGF at 1:10,000 for 90 minutes at room temperature followed by incubation with HRP-conjugated horse anti-mouse IgG at 1:7000 for 60 minutes at room temperature. There were four 5-minute washes with PBS containing 0.5% Tween 20 following each step. The blot was treated with chemiluminescence reagent (NEL-102; DuPont NEN, Boston, MA), according to the vendor and exposed against Kodak film (X-OMAT AR; Kodak, Rochester, NY) for 1 to 2 minutes. The intensity of the specific bands were quantified by scanning densitometry using a GS-300-scanner (Hoefer Scientific Instruments).

Results

Hind limbs from normal rats exhibited no joint swelling with typical arthritic scores ≤15% during the period of experiment. No apparent inflammatory changes were observed. Periosteum exhibited one to two layers of cells with fibrocyte morphology. Staining for bFGF was observed in blood vessels, proliferating chondrocytes in the growth plate, a small number of osteoblasts, and some scattered cells in loose connective tissue. In SCJs and periosteum, bFGF staining was limited to blood vessels (Figure 1a). PCNA immunoreactivity was found in <5% of periosteal cells (inner layer of periosteum) (data not shown). Although the BrdU labeling regimen labeled only one quarter of the proliferating fraction that stained for PCNA, the distribution patterns as well as the staining kinetics of both BrdU and PCNA cells were identical. Weak staining for PDGF-A was present in tendon and smooth muscle cells in blood vessels but essentially absent from periosteum, synovium, bone matrix, and carti-

lage (data not shown). Intense PDGF-A staining was only found in cytoplasm of megakaryocytes in bone marrow (Figure 3c) and in nerve fibers (data not shown). Joint tissue from arthritis-free rats 9 days after adjuvant inoculation is indistinguishable from that of control rats pathologically and immunohistologically (Table 1).

Three major pathological changes were readily observed during development of the articular inflammation: periarticular and intraarticular infiltration with inflammatory cells; erosion of cartilage, bone, and tendon; and osteogenesis. Neovascularization and chondrogenesis were also often seen. Of these changes, bone erosion and formation, in particular, exhibited a great extent of temporal overlapping with bone erosion dominating the early stage, whereas bone formation dominating the late stage (Table 1). Although staining for bFGF seemed to be related to both destructive and osteogenic processes, PDGF-A immunostaining, in contrast, was predominantly associated with bone formation.

On disease onset on days 11 to 13 the afflicted hind limbs showed apparent redness and swelling with typical arthritic scores of 30 to 60%. Histology indicated acute inflammation with extensive acellular exudation and mild to moderate cell infiltration in synovium and in loose connective tissue adjacent to joints and tendons in all afflicted limbs examined. No obvious formation of panni or synovial villi and erosion of joint or tendon were observed. The periosteum proximal to inflamed joints exhibited hypertrophy. Staining for bFGF, however, began to appear in three major areas in addition to blood vessels: periosteum (Figure 2a), SCJs, and scattered cells in inflamed loose connective tissue (Figure 1b). Although less than 10% of SCJs exhibited bone erosion, more than 60% of SCJs were stained for bFGF (Table 1, Figure 5). Western blot analysis also revealed a twofold increase in the bFGF level of the joint tissues (Figure 4). Double staining of PCNA/bFGF showed that PCNA and bFGF immunoreactivities were co-localized in lining synovium (Figure 1b), periosteum, and some capillaries (Figure 2a). Anti-PDGF-A exhibited the same staining pattern as that seen before onset.

The magnitude of swelling of an afflicted limb reached its peak between days 17 and 24 and remained unchanged for about 1 week. The typical arthritic score during days 17 to 20 was 60 to 80%. Increased inflammatory cell infiltration in synovium and progressive erosion of cartilage, subchondral bone, and tendon characterized pathological changes occurring by days 17 to 24. Histology showed an acute to subacute inflammation characterized by extensive infiltration of inflammatory cells,
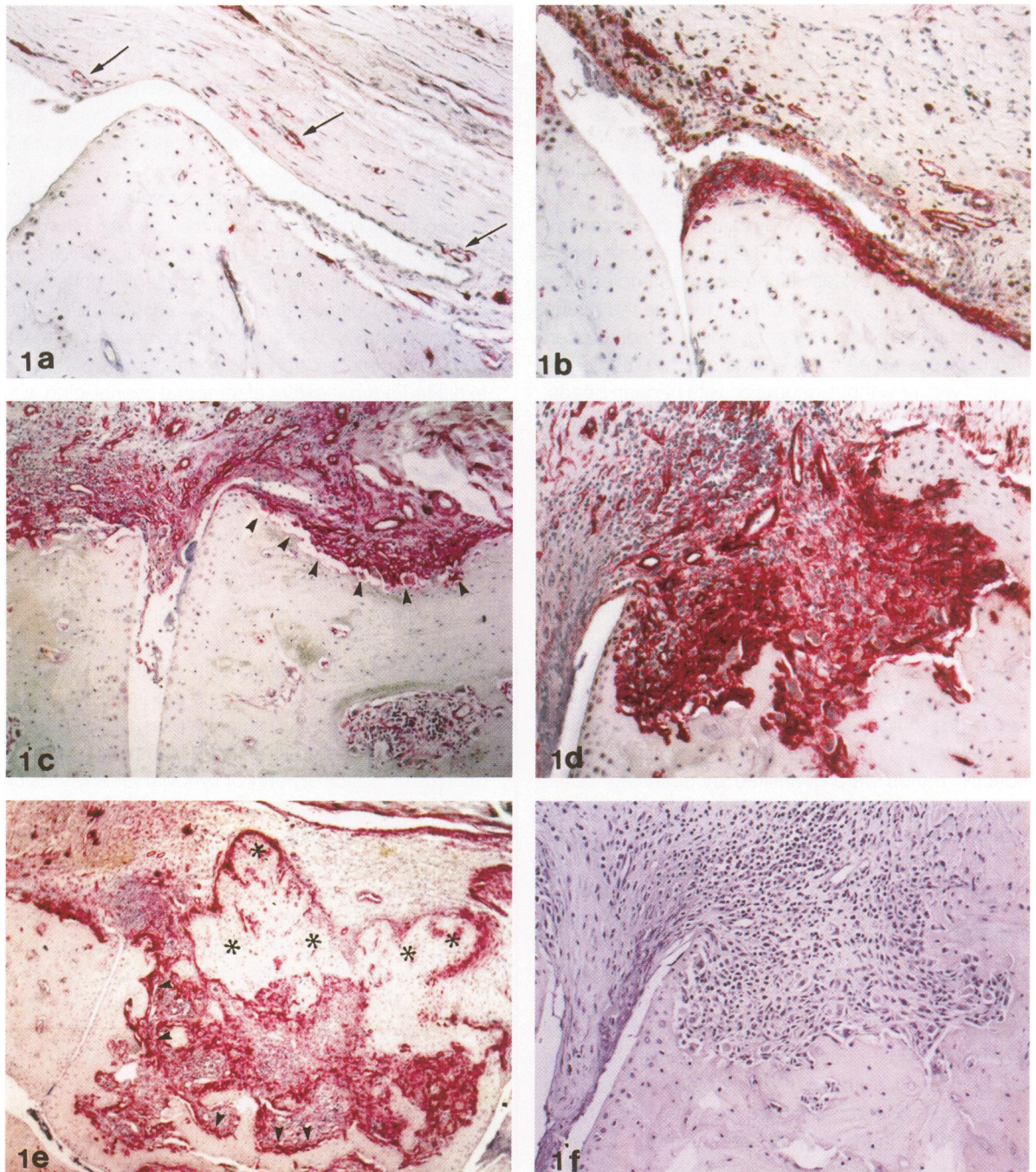
Figure 1. *Immunostaining of SCJs: staining for bFGF (pink) in normal SCJ is minimal and is mainly associated with blood vessels (arrows) (a), whereas increased bFGF staining is found at SCJ at early stage of inflammation (day 12) (b). Early bone erosion by a newly formed pannus was accompanied by strong bFGF staining (pink) of the pannus (day 17) (arrowheads) (c) Strong bFGF staining (pink) is seen throughout the pannus at the peak of erosion (day 23) (d). As the erosion progresses, the pannus invades into and replaces subchondral bone. Strong bFGF immunoreactivity remains at the pannus/bone junction (arrowhead) (e). Note the periosteal bone formation (stars) (e). Replacing the anti-bFGF and anti-PCNA with nonimmune antibodies for the first and second labeling abolishes the specific staining (f). Magnification: a–c and f ×200; e ×400.*

outgrowth of synovia, and formation of panni that progressively eroded tendon, subchondral bone, and cartilage (Figure 1, c and d). Periosteum proximal to afflicted joints exhibited dramatic hyperplasia and began to give rise to osteoid between the original

bone cortex and hyperplastic periosteum (Figure 2b). Intense staining for bFGF was found in newly formed panni, thickened periosteum, and capillaries in adjacent soft tissue (Figures 1, c and d and 2b). Although there was about a 20% increase in the number

of bFGF-positive SCJs compared with that on days 11 to 13, the increase in the number of SCJs exhibiting bone erosion was dramatic (more than 50%) (Figure 5). More than 80% of total SCJs exhibited staining for bFGF (Table 1, Figure 5). An increased number of PCNA-/BrdU-positive cells was also observed in the panni and periosteum (Figure 2b). PCNA and bFGF staining were highly co-localized in these regions (Figure 2, b and c, Table 1). The staining pattern of PDGF-A remained primarily unchanged except that weak to moderate PDGF-A staining was noticed within the area of the osteoid tissue.

Extensive subchondral bone destruction, active intramembranous bone formation, and the presence of PDGF-A immunoreactivity in the osteogenic tissue characterized the pathological changes observed on days 24 to 27. The majority of SCJs (>80%) demonstrated bone destruction and positive staining for bFGF (Figure 5). The subchondral bone was gradually replaced by invading panni that evolved into granular tissue containing inflammatory cells and multinucleated giant cells (Figure 1d). As a pannus continued to extend and expand into the subchondral region, bFGF staining became diminished in the connective tissue core of the expanded pannus. However, cells at the leading edge of the pannus continuously showed strong staining for bFGF (Figure 1e). Synovial tissue exhibited heavy infiltration, neovascularization, and hyperplasia as well as hypertrophy of lining synoviocytes. Intense immunostaining for bFGF was found in lining synoviocytes, with dendritic morphology, small blood vessels, and extracellular matrix in inflamed synovium (Figure 3a). A great percentage of lining synoviocytes showed nuclear staining for PCNA (≥50%) and BrdU (≥15%) (Figure 3a). Meanwhile, active periosteal bone formation along adjacent bone shaft was observed. The newly formed bone grew from the bone shaft and formed dactylate (finger-like) projections. Periosteum surrounding the newly formed bone consisted of highly cellular soft tissue with fibroblast-like cells and blood vessels that exhibited strong bFGF staining (Figure 2e). A great percentage of BrdU/PCNA-positive cells was found in the thickened periosteum and remained co-localized with bFGF immunoreactivity (Figure 2f). Increased staining for PDGF-A was apparent in the newly formed bone tissue, whereas the original bone matrix remained largely unstained (Figure 2, c and d).

Pathological changes seen on days 33 to 40 were marked by extensive osteogenesis and a gradual reduction in inflammatory infiltration along with a dramatic decrease in bFGF and PCNA/BrdU immunoreactivity. Histologically, subchondral bone of afflicted joints was largely destroyed and replaced with granu-

lar tissue, whereas the periosteal new bone expanded to form a large mass that stained strongly for PDGF-A. bFGF immunoreactivity in pannus and periosteum was greatly decreased, although weak to moderate staining for bFGF was still present in some of the blood vessels (Figure 2g). Western blot analysis also showed a decrease in bFGF in the inflamed limb to levels substantially below normal controls (Figure 4). A simultaneous decrease in the number of total cells and in the percentage of PCNA/BrdU-positive cells in the periosteum accompanied the reduction of bFGF (Figure 2e). In contrast, intense PDGF-A staining remained in the periosteal bone (data not shown). At the end of this period, granular tissue that had replaced the original subchondral bone gradually made a transition into granulation tissue with a greatly reduced number of infiltrated inflammatory cells and multinucleated giant cells. A transient local increase in bFGF but not PDGF-A staining in these areas was noticed. The granulation tissue then developed into woven bone, which was stained for PDGF-A (data not shown).

Despite the high incidence of polyarthritis in this model, about 10% of the adjuvant-treated rats remained arthritis free with joint scores ≤15% and showed no sign of inflammation (joint swelling, redness, cell infiltration, and bone erosion) until sacrifice (≥day 17). Moreover, in some adjuvant-treated rats only one hind limb was affected. In these arthritis-free hind limbs (n = 7) from adjuvant-treated rats, about 70% of SCJs exhibited increased staining for bFGF without apparent cell infiltration, pannus formation, bone destruction, or osteogenesis (data not shown). However, they exhibited an identical staining PDGF-A pattern as the limbs from nontreated rats.

Immunostaining was abolished in control sections using nonimmune antibodies (Figure 1f) or preabsorbed anti-bFGF and anti-PDGF-A. Although washing sections with buffer containing 2 M NaCl completely eliminated staining for bFGF, it did not affect staining for BrdU or PCNA. Possible cross-reaction between the primary and secondary antibodies for double labeling was excluded by using a medullary bone sample as a positive control in which staining for bFGF and PDGF-A was found in osteoclasts and megakaryocytes, respectively (Figure 3c). The specificity of anti-bFGF used for immunohistochemical staining was further confirmed by immunoblot analysis. On the blot analysis, all samples exhibited a specific band of about 17 kd with migration identical to that of human recombinant bFGF (Figure 4). Consistent with the immunohistochemical result, an increase in bFGF level was observed at the time of onset (day
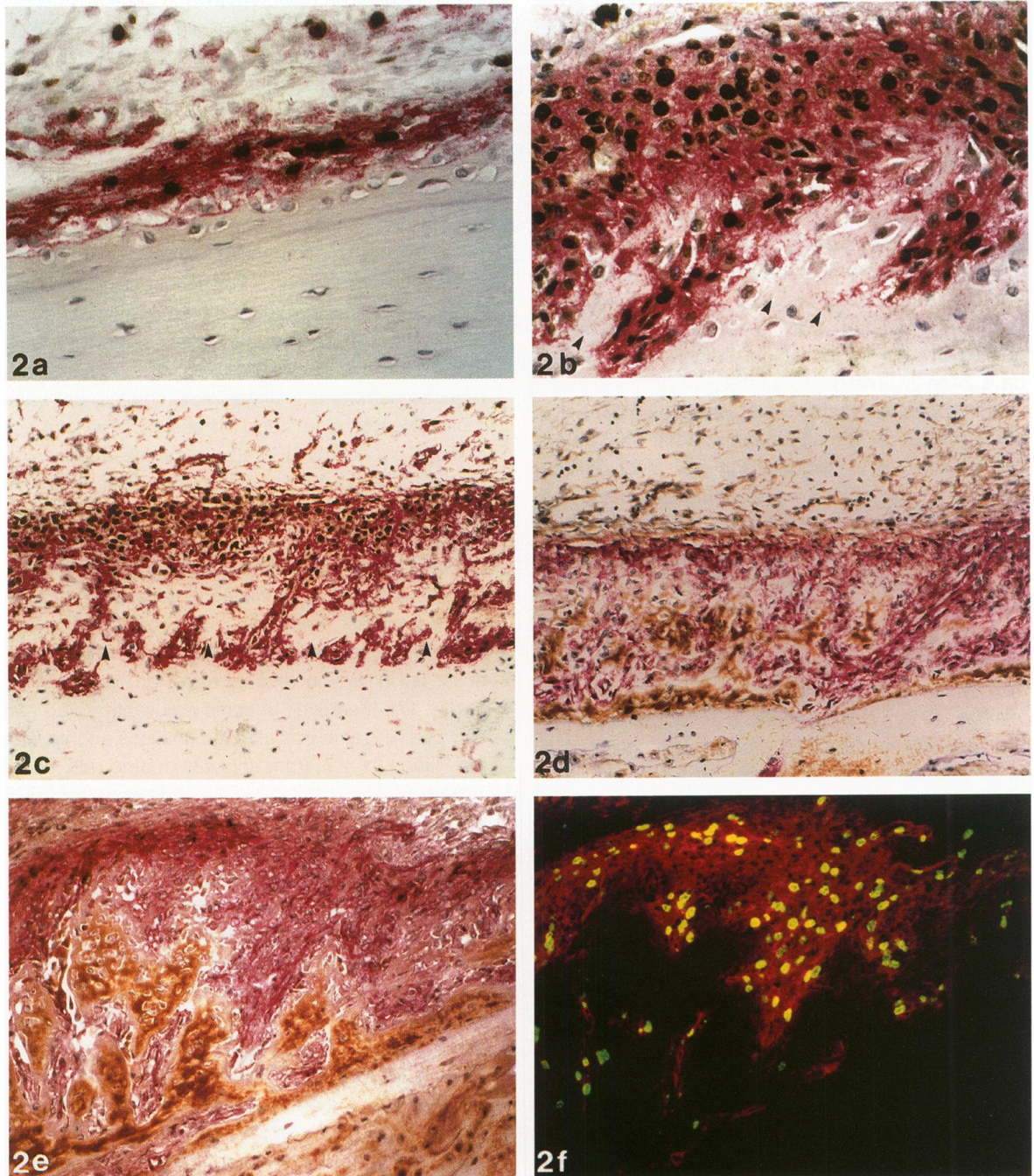
Figure 2. *Immunostaining of periosteum and osteogenic tissue: double staining shows the co-localization of bFGF (pink) and the cell proliferation marker, BrdU (black), in thickened periosteum (a). Increased staining for bFGF (pink) and PCNA (black) is found as periosteum undergoes hyperplasia (b) and begins to develop into osteoid (arrowhead in b). Periosteal hyperplasia was followed by formation of osteoid (arrowheads) as shown in (c) and (d). Note the co-localization of bFGF (pink) and PCNA (black) in the hyperplastic periosteum and staining for PDGF-A (brown) in osteoid (d). e and f show triple-labeled osteogenic tissue on day 24. The newly formed osteoid growing from original bone shaft is stained for PDGF-A (golden brown) and surrounded by thickened periosteum with bFGF staining (pink) (e). The same tissue field under fluorescence demonstrates localization of BrdU-positive cells (bright green) in the thickened periosteum (f). Note the reciprocal staining pattern of PDGF-A and bFGF (e) and the absence of both bFGF and PCNA/BrdU staining in the osteogenic tissue. g shows decreased bFGF (pink)/PCNA (dark brown, arrows) staining and cell number of periosteum (arrowheads) at late stage (day 40). Magnification a and b ×400; c–g ×200.*
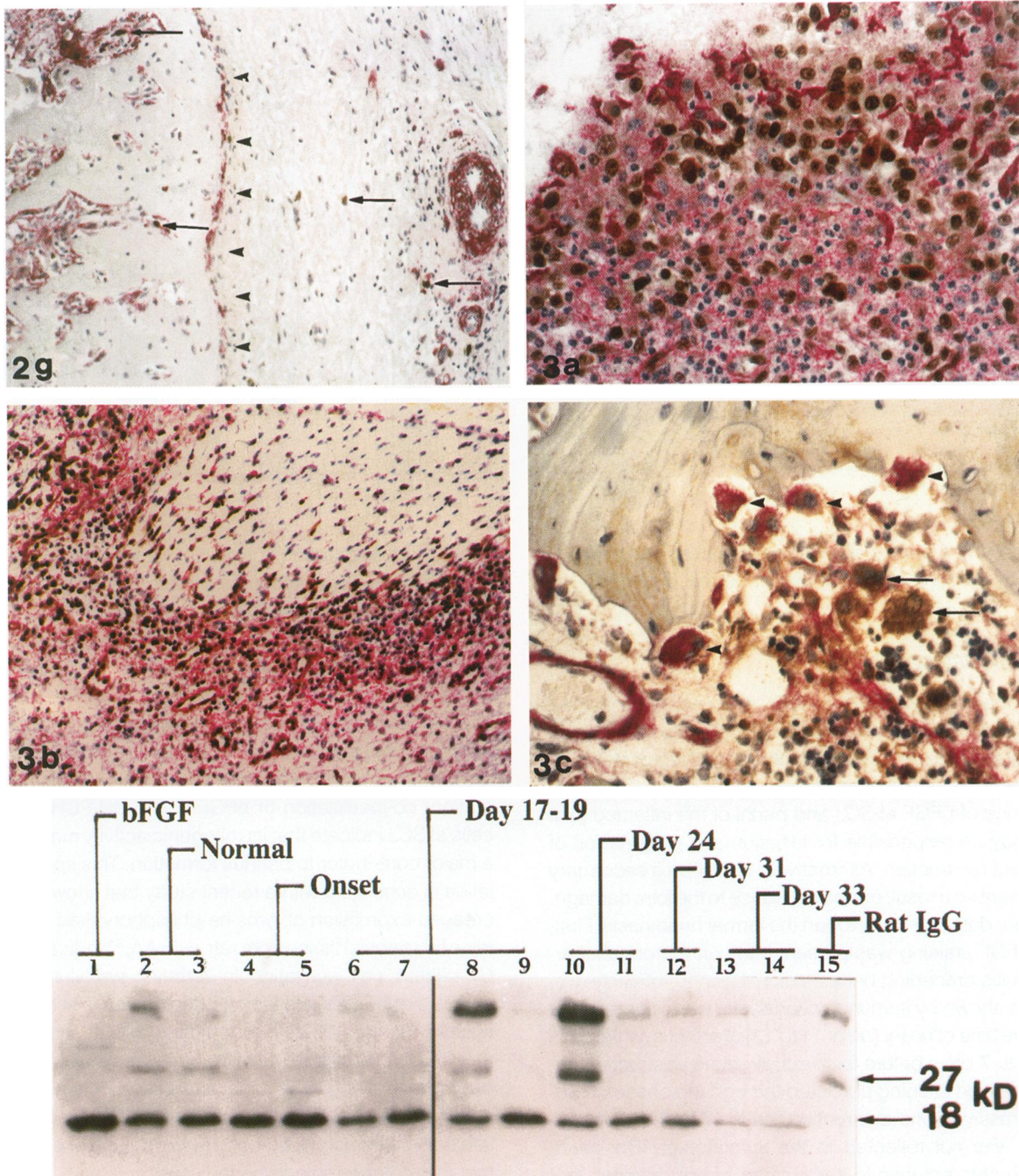
Figure 3. *Immunostaining of inflamed limbs with synovitis and tendinitis.* **a:** *shows double labeling of bFGF (pink) and PCNA (brown) in arthritic synovium. Increased bFGF staining is found both intracellularly and extracellularly in the inflamed synovium. Note that the majority of lining synoviocytes exhibit nuclear staining for PCNA.* **b:** *Demonstrates increased bFGF (pink) staining and PCNA (black) in an inflamed synovial sheath invading a tendon.* **c:** *Shows medullary bone sample as a positive control. Note that the positive staining for PDGF-A (brown) associated with megakaryocyte (arrows) and bFGF staining (pink) with blood vessel and osteoblasts (arrowheads) were mutually exclusive. Magnification* **a** *and* **c** *×400;* **b** *×200.*

Figure 4. *Western blot analysis of total joint tissue for bFGF. A specific band with an apparent molecular weight of 16 to 17 kd that exhibits identical migration as human recombinant bFGF (lane 1) is found in all joint samples (lanes 2 to 14). The high molecular weight bands (≥25 kd) result from a cross-reaction of contaminating endogenous rat immunoglobulin with the (HRP-conjugated horse anti-mouse) secondary antibody as shown in lane 15.*
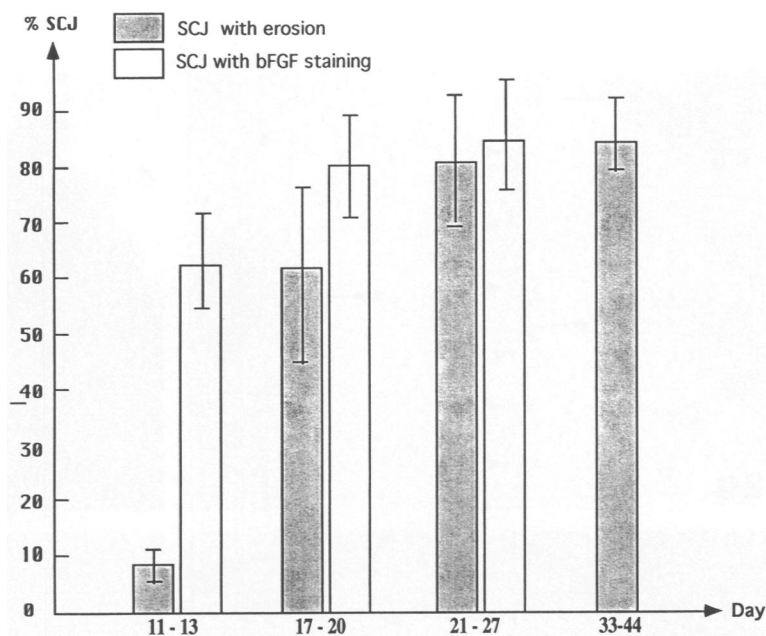
Figure 5. *Histogram shows the percentage of SCJs that exhibit bone erosion (closed box) and positive staining for bFGF (open box) during the course of AA. Determination of bFGF staining data on days 30 to 40 were not applicable due to massive destruction by invasive panni that completely replaced SCJs.*

13) and the level showed an apparent decrease on day 33 compared with that of normal (Figure 4).

Discussion

Localization of bFGF at the SCJ and panni in inflamed arthritic joints but not at the SCJ of joints from control rats, suggests that this multifunctional factor may play a role in the process of bone destruction. The presence of bFGF at SCJ and panni of the inflamed joint may be responsible for initiation and progression of joint destruction. Alternatively, it may be a secondary event as a result of local response to the joint damage. Our data seem to support the former hypothesis. First, bFGF staining was present early on the onset of arthritis preceding bone erosion. Second, bFGF levels, as shown by immunoblot analysis, were increased at the time of onset (days 11 to 13) of arthritis, which was 5 to 7 days before microscopic bone destruction. Increased staining persisted through the phase of progressive bone destruction (days 17 to 24), although it was not reflected in the immunoblot. The much greater increase in the number of lymphocytes that did not express bFGF may have diluted the specific immunoreactivity of bFGF in tissue extracts during this period. In contrast, PDGF-A staining was not observed to increase in afflicted joints until active osteogenesis took place 7 to 10 days after onset, when extensive joint destruction had already occurred. Third, bFGF immunoreactivity was also present in periosteum proximal to SCJ where no bone erosion was apparent. In fact, active osteogenesis was ob-

served in these areas, suggesting increased bFGF expression is not a secondary event resulting from bone destruction. It has been shown that bFGF is a potent inducer of a variety of metalloproteinases[8,9] and plasminogen activator.[10] Increased expression of metalloproteinases in rheumatoid synovium has also been shown by both immunohistochemistry and *in situ* hybridization.[30-33] Furthermore, the invasive growth of synovial panni requires active cell proliferation; co-localization of bFGF and BrdU/PCNA in cells at SCJ indicate that its mitogenic activity may be a major contributor to pannus formation. This speculation is consistent with a recent study that shows increased expression of tyrosine-phosphorylated proteins by synovial tissue from rats with AA,[34] indicating GF-related cell activation in arthritic synovium. It seems that bFGF's role in bone destruction is at least twofold. It may directly or indirectly initiate or up-regulate expression of metalloproteinases that in turn degrade proteoglycan and collagens, ultimately leading to joint destruction. In addition, it may stimulate cell proliferation leading to the formation of panni that invade and replace bone tissue.

Studies have also shown that bFGF stimulates bone formation *in vitro* and *in vivo*.[18-21] Increased bFGF expression throughout the healing process of bone fracture has also been reported.[35] Our observations are consistent with these findings and strongly suggest that bFGF may also function as an osteotrophic factor in periosteal bone formation during adjuvant arthritis. First, strong bFGF staining was always found in the periosteum adjacent to newly

formed bone tissue during the phase of active osteogenesis (days 17 to 27). Second, bFGF was colocalized with BrdU/PCNA at the thickened periosteum, suggesting its involvement in active cell proliferation in this region. Furthermore, both cell number and staining for bFGF and BrdU/PCNA exhibited a drastic decrease as the disease process progressed into remission (days 33 to 40). Such tightly coupled staining patterns strongly implicated bFGF in the periosteal osteogenesis observed in this arthritic animal model. In contrast, PDGF-A staining showed a quite different temporal and spatial pattern in this region. Its presence lagged about 1 week behind that of bFGF and was restricted to the osteoid where no cell proliferation was detected. Such temporal and spatial differences may reflect a functional coordination between these GFs. The simplest scenario is that during osteogenesis, increased bFGF with its mitogenic and angiogenic effects may have led to active periosteal cell proliferation for the formation and expansion of the osteogenic tissue. The subsequent expression of PDGF-A may be responsible for continuation of the osteogenic process, ie, differentiation, maturation, and calcification. The immunostaining for both BrdU and PCNA in the nuclei of hyperplastic synovium observed in this study is consistent with our previous observation made in human rheumatoid synovium that local cell proliferation contributes significantly to synovial hyperplasia.[28]

Our observations are consistent with other studies suggesting that bFGF may have dual effects during articular inflammation (see earlier text). One important question is what decides whether bone destruction or osteogenesis is elicited by locally increased bFGF expression. Two major factors may underlie such distinct tissue responses: the intrinsic difference of different types of target cells and the difference in microenvironments at SCJ and periosteum along the bone shaft. SCJ differs from the proximal periosteum in both of these two aspects. First, there are two major types of cells in SCJs that are absent in proximal periosteum: chondrocytes and synoviocytes. Both of them are important sources of metalloproteinases and are major targets of bFGF.[22,36,37] Second, dramatic infiltration of inflammatory cells occurs in synovium at SCJs and around tendon, whereas cell infiltration along bone shaft is usually mild, if present. The inflammatory cells are rich sources of a variety of cytokines such as IL-1 and TNF-α, which are known to collaborate functionally with bFGF to up-regulate expression of matrix proteinases and prostanoid production by chondrocytes and synoviocytes[8, 11–13] ultimately resulting in bone destruction (see Introduction). Increased bFGF at proximal periosteum, on the

other hand, may target periosteal cells and with collaboration of a different set of GFs such as PDGF-A induce bone formation. In support of this are the findings that intraarticular infusion of bFGF alone promotes cartilage repair, whereas co-injection of bFGF and IL-1 induces cartilage degradation in rabbits.[17,37] Taken together, our observations and those of others suggest that the microenvironment is critical in programming cellular responses to bFGF and that collaboration of a number of growth factors may be important during the disease process.

The concomitant presence of increased bFGF expression and onset of the articular inflammation does not mean that bFGF initiated the disease process. In fact, absence of increased bFGF staining before the onset on day 9 and of articular inflammation in arthritis-free limbs from arthritic rats, despite increased bFGF staining, suggests that bFGF is not an initiating factor of the inflammation. Other GFs such IL-1 and TNF-α are more likely to the candidate(s).

Functional overlap is known to exist among certain multifunctional GFs. Both PDGF and bFGF, for example, are mitogenic for mesenchymal cells; both potentiate IL-1-induced synthesis of metalloproteinase by chondrocytes,[8,38,39] both accelerate the wound-healing process and the repair of bone fractures,[35] and both stimulate osteoblast proliferation and induce bone formation *in vitro* and *in vivo*.[40–42] It also seems a common occurrence that some GFs exhibit tissue co-localization. For example, immunolocalization reveals similar distribution patterns of acidic FGF, PDGF-B, and transforming growth factor-β in synovium from patients with RA and Lewis rats with experimental arthritis when a high concentration of the specific primary antibodies (20 to 50 μg/ml) and the ABC method were used.[43–45] More recently, co-localization of acidic FGF and PDGF-B with phosphotyrosine-containing protein is reportedly present in arthritic joint tissue from humans and rats.[34] In contrast, our studies indicate a striking disparity in the temporal and spatial expression patterns of two GFs with similar functions *in vitro*. These differences can, of course, be attributed to the distinct GFs that were detected in each report. The reciprocal nature of the staining that we detect argues strongly for unique roles for each GF. More importantly, our study related the GF's expression with pathological changes in the course of the articular inflammation and suggested that bFGF may play an important role in joint destruction and new bone formation. Although functional collaboration of different GFs exists in articular inflammation, specific GFs may be responsible for a specific aspect of the disease process. Modulation of the expression or activity of a specific growth

factor at an appropriate stage may effectively modulate the pertinent disease process. Experiments are currently in progress to test this hypothesis by *in vivo* modulation of bFGF activity.

Acknowledgments

References

1. Brennan FM, Field M, Chu CQ, Feldmann M, Maini RN: Cytokine expression in rheumatoid arthritis (Review). Br J Rheumatol 1991, 30 (Suppl 1):76–80
2. Lipsky PE, Davis LS, Cush JJ, Oppenheimer-Marks N: The role of cytokines in the pathogenesis of rheumatoid arthritis. Springer Semin Immunopathol 1989, 11: 123–162
3. Finklestein SP, Apostolides PJ, Caday CG, Prosser J, Philips MF, Klagsbrun M: Increased basic fibroblast growth factor (bFGF) immunoreactivity at the site of focal brain wounds. Brain Res 1988, 460:253–259
4. Broadley KN, Aquino AM, Hicks B, Ditesheim JA, McGee GS, Demetriou AA, Woodward SC, Davidson JM: Growth factors bFGF and TGB beta accelerate the rate of wound repair in normal and in diabetic rats. Int J Tissue React 1988, 10:345–353
5. Broadley KN, Aquino AM, Woodward SC, A B-S, Sato Y, Rifkin DB, Davidson JM: Monospecific antibodies implicate basic fibroblast growth factor in normal wound repair. Lab Invest 1987, 61:571–575
6. Burges WH, Maciag T: The heparin-binding (fibroblast) growth factor family of proteins (Review). Annu Rev Biochem 1989, 58:575–606
7. Gospodarowicz D: Fibroblast growth factor. Oncogenesis 1989, 1:1–25
8. Bandara G, Lin CW, Georgescu HI, Mendelow D, Evans CH: Chondrocyte activation by interleukin-1: analysis of the synergistic properties of fibroblast growth factor and phorbol myristate acetate. Arch Biochem Biophys 1989, 274:539–547
9. Chua CC, Chua BH, Zhao ZY, Krebs C, Diglio C, Perrin E: Effect of growth factors on collagen metabolism in cultured human heart fibroblasts. Connect Tissue Res 1991, 26:271–281
10. Saksela O, Rifkin DB: Cell-associated plasminogen activation: regulation and physiological functions (Review). Annu Rev Cell Biol 1988, 4:93–26
11. Chandrasekhar S, Harvey AK: Induction of interleukin-1 receptors on chondrocytes by fibroblast growth factor: a possible mechanism for modulation of interleukin-1 activity. J Cell Physiol 1989, 138:236–246
12. Unemori EN, Hibbs MS, Amento EP: Constitutive expression of a 92-kD gelatinase (type V collagenase) by rheumatoid synovial fibroblasts and its induction in normal human fibroblasts by inflammatory cytokines. J Clin Invest 1991, 88:1656–1662
13. Chin JE, Hatfield CA, Krzesicki RF, Herblin WF: Interactions between interleukin-1 and basic fibroblast growth factor on articular chondrocytes: effects on cell growth, prostanoid production, and receptor modulation. Arthritis Rheum 1991, 34:314–324
14. Goddard DH, Grossman SL, Newton R: Polypeptide growth factors augment interleukin 1-induced release of prostaglandin E2 by rheumatoid arthritis synovial cells in vitro. Cytokine 1990, 2:294–299
15. Stevens TM, Chin JE, McGowan M, Giannaras J, Kerr JS: Phospholipase A2 (PLA2) activity in rabbit chondrocytes. Agents Actions 1989, 27:385–387
16. Stimpson SA, Dalldorf FG, Otterness IG, Schwab JH: Exacerbation of arthritis by IL-1 in rat joints previously injured by peptidoglycan-polysaccharide. J Immunol 1988, 140:2964–2969
17. Stevens P, Shatzen EM: Synergism of basic fibroblast growth factor and interleukin-1 beta to induce articular cartilage-degradation in the rabbit. Agents Actions 1991, 34:217–219
18. Noff D, Pitaru S, Savion N: Basic fibroblast growth factor enhances the capacity of bone marrow cells to form bone-like nodules in vitro. FEBS Lett 1989, 250:619–621
19. Aspenberg P, Lohmander LS: Fibroblast growth factor stimulates bone formation: bone induction studied in rats. Acta Orthopaed Scand 1989, 60:473–476
20. Canalis E, Centrella M, McCarthy T: Effects of basic fibroblast growth factor on bone formation in vitro. J Clin Invest 1988, 81:1572–1577
21. Mayahara H, Ito T, Nagai H, Miyajima H, Tsukuda R, Taketomi S, Mizoguchi J, Kato K: In vivo stimulation of endosteal bone formation by basic fibroblast growth factor. Growth Factors 1993, 9:73–80
22. Melnyk VO, Shipley GD, Sternfeld MD, Sherman L, Rosenbaum JT: Synoviocytes synthesize, bind, and respond to basic fibroblast growth factor. Arthritis Rheum 1990, 33:493–500
23. Goddard DH, Grossman SL, Newton R, Clark MA, Bomalaski JS: Regulation of synovial cell growth: basic fibroblast growth factor synergizes with interleukin 1 beta stimulating phospholipase A2 enzyme activity, phospholipase A2 activating protein production and release of prostaglandin E2 by rheumatoid arthritis synovial cells in culture. Cytokine 1992, 4:377–384
24. McCartney-Francis N, Allen JB, Mizel DE, Albina JE, Xie Q-W, Nathan CF, Wahl SM: Suppression of arthritis by an inhibitor of nitric oxide synthase. J Exp Med 1993, 178:749–754
25. Goureau O, Lepoivre M, Becquet F, Courtois Y: Differential regulation of inducible nitric oxide synthase by fibroblast growth factors and transforming growth factor β in bovine retinal pigmented epithelial cells: inverse correlation with cellular proliferation. Proc Natl Acad Sci USA 1993, 90:4276–4280
26. Taurog JD, Argentieri DC, McReynolds RA: Adjuvant arthritis. Methods Enzymol 1988, 162:339–355

27. Goldings EA, Jasin HE: Arthritis and autoimmunity in animals. In Arthritis and Allied Conditions, ed 11. Edited by McCarty DJ, Lea & Febiger, 1989, pp 465–481

28. Qu Z, Garcia CH, O'Rourke LM, Planck SR, Kohli M, Rosebaum JT: Local proliferation of fibroblast-like synoviocytes contributes to synovial hyperplasia: results of proliferating cell nuclear antigen/cycclin, c-myc and nucleolar organizer staining. Arthritis Rheum 1994, 37: 212–220

29. Wray W, Boulikas T, Wray VP, Hancock R: Silver staining of protein in polyacrylamide gels. Anal Biochem 1981, 118:197–203

30. Gravallese EM, Darling JM, Ladd AL, Katz JN, Glimcher LH: In situ hybridization studies of stromelysin and collagenase messenger RNA expression in rheumatoid synovium. Arthritis Rheum 1991, 34:1076–1083

31. Firestein GS, Paine MM: Stromelysin and tissue inhibitor of metalloproteinases gene expression in rheumatoid arthritis synovium. Am J Pathol 1992, 140:1309–1314

32. McCachren SS: Expression of metalloproteinases and metalloproteinase inhibitor in human arthritic synovium. Arthritis Rheum 1991, 34:1085–1093

33. Okada Y, Gonoji Y, Nakanishi I, Nagase H, Hayakawa T: Immunohistochemical demonstration of collagenase and tissue inhibitor of metalloproteinases (TIMP) in synovial lining cells of rheumatoid synovium. Virchows Arch B Cell Pathol 1990, 59:305–312

34. Sano S, Engleka K, Mathern P, Hla T, Crofford LJ, Remmers EF, Jelsema CL, Goldmuntz E, Maciag T, Wilder RL: Coexpression of phosphotyrosine-containing proteins, platelet-derived growth factor-B, and fibroblast growth factor-1 in situ in synovial tissues of patients with rheumatoid arthritis and Lewis rats with adjuvant or streptococcal cell wall arthritis. J Clin Invest 1993, 91: 553–565

35. Bolander ME: Regulation of fracture repair by growth factors. Proc Soc Exp Biol Med 1992, 200:165–170

36. Osborn KD, Trippel SB, Mankin HJ: Growth factor stimulation of adult articular cartilage. J Orthop Res 1989, 7:35–42

37. Cuevas P, Burgos J, Baird A: Basic fibroblast growth factor (FGF) promotes cartilage repair in vivo. Biochem Biophys Res Commun 1988, 156:611–618

38. Harvey AK, Stack ST, Chandrasekhar S: Differential modulation of degradative and repair responses of interleukin-1-treated chondrocytes by platelet-derived growth factor. Biochem J 1993, 292:129–136

39. Smith RJ, Justen JM, Sam LM, Rohloff NA, Ruppel PL, Brunden MN, Chin JE: Platelet-derived growth factor potentiates cellular responses of articular chondrocytes to interleukin-1. Arthritis Rheum 1991, 34:697–706

40. Canalis E, McCarthy TL, Centrella M: Effects of platelet-derived growth factor on bone formation in vitro. J Cell Physiol 1989, 140:530–537

41. Pfeilschifter J, Oechsner M, Naumann A, Gronwald RG, Minne HW, Ziegler R: Stimulation of bone matrix apposition in vitro by local growth factors: a comparison between insulin-like growth factor I, platelet-derived growth factor, and transforming growth factor beta. Endocrinology 1990, 127:69–75

42. Risto O, Wahlstrom O, Abdiu A, Walz T: Effect of platelet derived growth factor on heterotopic bone formation in rats. Acta Orthopaed Scand 1991, 62:49–51

43. Remmers EF, Sano H, Lafyatis R, Case JP, Kumkumian GK, Hla T, Maciag T, Wilder RL: Production of platelet derived growth factor B chain (PDGF-B/c-sis) mRNA and immunoreactive PDGF B-like polypeptide by rheumatoid synovium: coexpression with heparin binding acidic fibroblast growth factor-1. J Rheumatol 1991, 18:7–13

44. Sano H, Forough R, Maier JA, Case JP, Jackson A, Engleka K, Maciag T, Wilder RL: Detection of high levels of heparin binding growth factor-1 (acidic fibroblast growth factor) in inflammatory arthritic joints. J Cell Biol 1990, 10:1417–1426

45. Lafyatis R, Thompson NL, Remmers EF, Flanders KC, Roche NS, Kim S-J, Case JP, Sporn MB, Roberts AB, Wilder RL: Transforming growth factor-β production by synovial tissues from rheumatoid patients and streptococcal cell wall arthritic rats: studies on secretion by synovial fibroblast-like cells and immunohistologic localization. J Immunol 1989, 143:1142–1148

46. Root LL, Shipley GD: Human dermal fibroblasts express multiple bFGF and aFGF proteins. In Vitro Cell Dev Biol 1991, 27A:815–822

47. Ansel JC, Tiesman JP, Olerud JE, Krueger JG, Krane JF, Tara DC, Shipley GD, Gilbertson D, Usui ML EHC: Human keratinocytes are major source of cutaneous platelet-derived growth factor. J Clin Invest 1993, 92: 617–678